S31-014

Energy transfer in the CP43 and CP47 complexes of photosystem II

FL de Weerd, IHM van Stokkum, JP Dekker, H van Amerongen, R van Grondelle

Department of Biophysics and Physics of Complex Systems, Division of Physics and Astronomy, Faculty of Sciences, Vrije Universiteit, De Boelelaan 1081, 1081 HV Amsterdam, The Netherlands. Fax (+31) 20 4447999; E-mail: weerd@nat.vu.nl

Keywords: dynamics, transient-absorption spectroscopy, CP43, CP47, photosystem II

Introduction

The light-harvesting complexes CP43 and CP47 are part of the core of photosystem II (PSII). Their main function is to funnel excitation energy into the reaction center (RC). The crystal structure of the PSII core complex of the cyanobacterium *Synechococcus elongatus* was published recently at a resolution of 3.8 Å (Zouni et al., 2001).
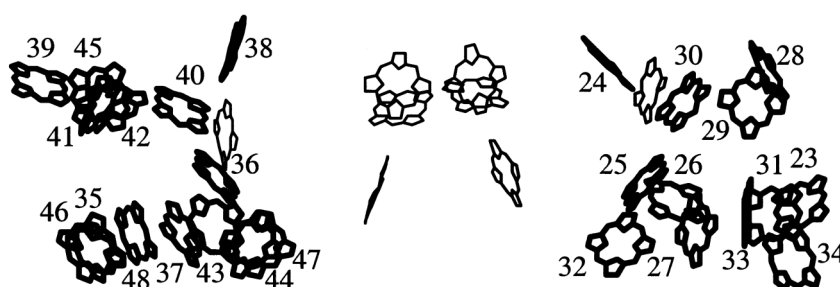

Fig. 1. Structure of the monomeric PSII core complex viewing along the membrane plane (Zouni et al., 2001). Luminal side is top, stromal side is bottom. CP47 is on the left, the RC in the middle, and CP43 on the right.

The 12 chlorophylls (Chls) in CP43 and the 14 Chls in CP47 are organized in two layers near the stromal and the luminal sides of the membrane. Here we present a full investigation of excitation energy transfer (EET) dynamics in isolated CP43 and CP47 complexes at 77K with a time resolution of ~140 fs. We simulated the observed dynamics on the basis of calculated absorption spectra.

Materials and methods

CP43 and CP47 were purified from spinach (Groot et al., 1995; Groot et al., 1999). Magic angle polarized data were recorded with a femtosecond spectrophotometer (Gradinaru et al., 2000). The obtained spectra were fitted with a global analysis fitting program (Van Stokkum et al., 1994). An irreversible sequential model with increasing lifetimes was assumed where each species associated difference spectrum (SADS) evolves into the next one. Note that these SADS in general reflect mixtures of states and are used as a means to describe the spectral evolution. The instrument response function was described by a Gaussian (fwhm 0.14 ps).

Results and discussion

Sub-picosecond transient absorption in CP43 and CP47

The 77K absorption spectra in the Q_y region of the purified CP43 and CP47 antenna complexes (thinner lines in Fig. 4) are characterized by a set of transitions at 660, 669, ~679 and ~682.5 nm (CP43) and at 661, 670, 677, 683 and 690 nm (CP47). Absorption difference

spectra were measured at 77K upon excitation around 671 nm (CP43) and 670 nm (CP47). The bandwidth of excitation was 8 nm (fwhm). To avoid annihilation, the excitation energy was kept low (~1.5 nJ/pulse).

Experimentally observed traces in CP43 are displayed in Fig. 2*A* (solid) together with the result of a global analysis fit to the data (dashed). Three SADS were required for this global fit (Fig. 2*B)*. The dotted spectrum in Fig. 2*B* represents the fitted coherent coupling between pump and probe pulses. The first SADS (solid) represents the absorption difference spectrum at time zero and shows a bleaching/stimulated emission (SE) at 671 nm. The second SADS (dashed) arises from the first with a 0.4 ps time constant. On this timescale, about half of the bleaching/SE at 671 nm is lost and transferred to a relatively sharp bleaching/SE component at 682 nm. The second SADS is then replaced by the third SADS (dot-dashed) with a 3.4 ps time constant. Most of the remaining bleaching/SE at 671 nm is lost and further builds up at 682 nm.

Experimentally observed traces in CP47 are displayed in Fig. 3*A* (solid), together with the result of a global analysis fit to the data (dashed). Four SADS were required for this fit (Fig. 3*B*), of which the first three are strongly reminiscent of the three SADS needed to describe the spectral evolution in CP43. The first SADS (Fig. 3*B*, solid) represents the absorption difference spectrum at time zero, and exhibits a broad bleaching/SE at 672 nm. The fitted coherent coupling between pump and probe pulses (dotted) imposes some difficulty in the precise fitting of the first SADS because of the somewhat faster spectral evolution that takes place in CP47: The first SADS (solid) is replaced by the second SADS (long-dashed) with a time constant of 0.2 ps. The bleaching/SE at 672 nm state is almost completely lost with this time constant and replaced by two bands at 677 and 683 nm. The third SADS (short-dashed) arises from the second SADS with a time constant of 1.7 ps and describes the consecutive transfer from the 677 nm component to the 683 nm component. The fourth SADS (dot-dashed) arises then with a much longer time constant (17 ps) and is associated with a partial relaxation from the Chls that were bleached at 683 nm to a Chl absorbing at even lower energy. The fourth SADS peaks at 685 nm and is asymmetric (fwhm 11 nm).
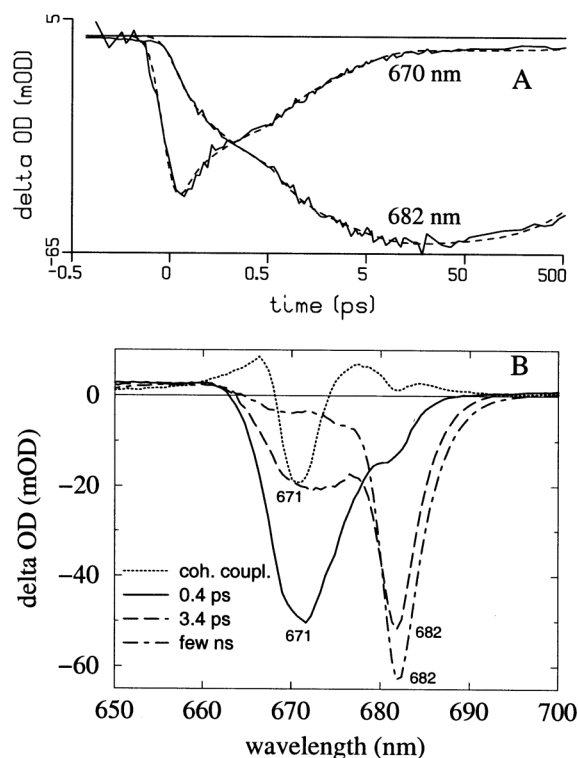

Fig. 2. (*A*) Traces recorded at 670 nm and 682 nm after 671 nm excitation of CP43 (solid) and global analysis fit (dashed), corrected for the dispersion. Note that the time-axis is linear between -0.5 and 0.5 ps and logarithmic at later delay times. (*B*) SADS resulting from the global fit. Each spectrum evolves with the given time constant into the next one.

Modelling the absorption properties of CP43 and CP47

That excitonic interactions may play an important role in determining the spectroscopic features in CP43 and CP47 can be inferred from the intense and conservative circular dichroism spectra that both complexes exhibit (Kwa et al., 1994; Groot et al., 1999). The crystal structure of the PSII core (Zouni et al., 2001) allows us to obtain estimates for the excitonic couplings. However, from this structure only the orientations of the normals to each Chl plane is known. Linear dichroism experiments on CP43 (Groot et al., 1999) and CP47 (De Weerd, unpublished observations) suggest that most oscillator strength is oriented at an angle to the normal of the membrane plane larger than the magic angle, except for the transition at 690 nm in CP47. Therefore we have put all the Q_y transitions in the plane of the membrane (it will appear that all main features in the calculated absorption spectra remain preserved when keeping all Q_y dipoles at an angle to the normal of the membrane plane larger than the magic angle). With this information, 'real' absorption spectra were calculated following a Monte Carlo procedure. Site energies were taken from a Gaussian centered at 14,925 cm^{-1} (670 nm) and with a fwhm of 200 cm^{-1}. The couplings between any pair of Chls were then calculated using the dipole-dipole approximation and an effective oscillator strength of Chl a of 24 D^2 was used.

For CP43, the calculated absorption spectrum bears an overall resemblance to the experimental spectrum (see Fig. 4), i.e. both contain a major peak near 669 nm, a shoulder near 661 nm and at least one red shifted transition in the 680 nm region, in approximately the right ratio. It follows that the intense band near 669 nm has equal contributions from stromal and luminal sides, while the single exciton transition in the red is due to stromal absorption (coupling between Chls 23, 27 and 33).

Also for CP47, the calculated absorption spectrum bears a resemblance to the experimental spectrum (see Fig. 4). The luminal part of CP47 has two additional Chls (nr. 39 and 45) compared to CP43, and both are involved in
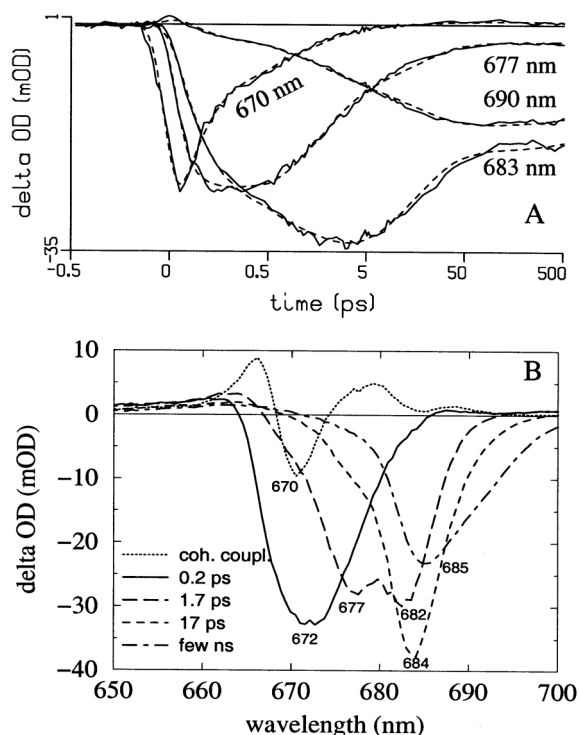

Fig. 3. (*A*) Traces recorded at 670, 677, 683 and 690 nm after 670 nm excitation of CP47 (solid) and global analysis fit (dashed), corrected for the dispersion. Note that the time-axis is linear between -0.5 and 0.5 ps and logarithmic at later delay times. (*B*) SADS resulting from the global fit. Each spectrum evolves with the given time constant into the next one.
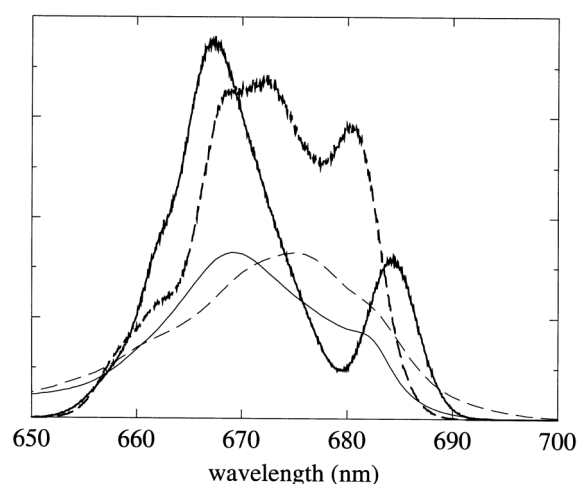

Fig. 4. Experimental absorption at 77K (thinner lines) and simulated absorption (thicker lines) of CP43 (solid) and CP47 (dashed).

strong pairwise interactions (Chl 39 with 42 and Chl 45 with 41). In our simulation, the Chl 44-47 pair on the stromal side and the 41-45 pair on the luminal side contribute mostly to the third and fourth lowest exciton level, and may give rise to the 677 nm band. The Chl 35-48 pair on the stromal side and the 39-42 pair on the luminal side contribute to the two lowest exciton levels, and may give rise to the 683 nm band.

Linking structure and excited-state dynamics

Upon exciting CP43 around 671 nm, we observed that half the excitations of the 670 nm component are transferred to the 682 nm component on a 0.4 ps timescale, and the other half on a 3 ps timescale. We assign the 0.4 ps time to a relaxation to the lowest state within the stromal side of the membrane and the 3 ps time to relaxation from the luminal to the stromal side. To estimate if the observed rates are consistent with the structure we have calculated the rate of energy transfer according to the Förster equation (Gradinaru et al., 1998), which will provide a reasonable estimate for weakly-coupled pigments. Assuming all the transition dipole moments to be oriented in the plane of the membrane, the fastest inter-layer rates are ~3 ps (between Chl 30 and 27 and also between 29 and 31), in agreement with our interpretation.

Upon exciting CP47 around 670 nm, we observed a transfer to the 677 and 683 nm components with a 0.2 ps time constant. Using the Förster equation, it follows that most of the Chls within the stromal layer are interconnected with subpicosecond energy transfer times. It also follows that within the luminal side not much subpicosecond energy transfer can occur. Therefore, we propose that the observed 0.2 ps rate reflects relaxation within the stromal side. The 677 nm component was shown to transfer its excitation energy to the 683 nm component on a 2 ps timescale. We calculated a 1.6 ps transfer time between the two luminal Chls 41 and 42, and a 1.4 ps time between Chl 40 and 42. The fastest calculated inter-layer rate was 3 ps (between Chls 37 and 40). We conclude that following the ultrafast relaxation on the stromal side, the observed 2 ps phase represents relaxation to the calculated lowest state, either the Chl 39-42 pair on the luminal or the Chl 35-48 pair on the stromal side.

References

Gradinaru CC, Özdemir S, Gülen D, Van Stokkum IHM, Van Grondelle R, Van Amerongen H (1998) *Biophysical Journal* **75**, 3064-3077.

Gradinaru CC, Van Stokkum IHM, Pascal AA, Van Grondelle R, Van Amerongen H (2000) *Journal of Physical Chemistry B* **104***, 9330-9342.

Groot M-L, Peterman EJG, Van Stokkum IHM, Dekker JP, Van Grondelle R (1995) *Biophysical Journal* **68**, 281-290.

Groot M-L, Frese RN, De Weerd FL, Bromek K, Pettersson Å, Peterman EJG, Van Stokkum IHM, Van Grondelle R, Dekker JP (1999) *Biophysical Journal* **77**, 3328-3340.

Kwa SLS, Völker S, Tilly NT, Van Grondelle R, Dekker JP (1994) *Photochemistry and Photobiology* **59***, 219-228.

Van Stokkum IHM, Scherer T, Brouwer AM, Verhoeven JW (1994) *Journal of Physical Chemistry B* **98**, 852-866.

Zouni A, Witt H-T, Kern J, Fromme P, Krauss N, Saenger W, Orth P (2001) *Nature* **409**, 739-743.